Carbohydrate Polymers 289 (2022) 119441

Contents lists available at ScienceDirect

Carbohydrate Polymers

journal homepage: www.elsevier.com/locate/carbpol

The development of a 3D printable chitosan-based copolymer with tunable properties for dentoalveolar regeneration

Mehdi Salar Amoli [a,b], Resmi Anand [a,c,d], Mostafa EzEldeen [b,e], Paulo Alexandre Amorim [a,c], Liesbet Geris [c,f,g], Reinhilde Jacobs [b,h], Veerle Bloemen [a,c,*]

[a] Surface and Interface Engineered Materials (SIEM), Campus Group T, KU Leuven, Andreas Vesaliusstraat 13, 3000 Leuven, Belgium
[b] OMFS IMPATH Research Group, Faculty of Medicine, Department of Imaging and Pathology, KU Leuven and Oral and Maxillofacial Surgery, University Hospitals Leuven, Kapucijnenvoer 33, 3000 Leuven, Belgium
[c] Prometheus, Division of Skeletal Tissue Engineering Leuven, KU Leuven, Leuven, Belgium
[d] Inter University Centre for Biomedical Research and Super Speciality Hospital, Mahatma Gandhi University Campus at Thalappady, Kottayam, Kerala 686009, India
[e] Department of Oral Health Sciences, KU Leuven and Paediatric Dentistry and Special Dental Care, University Hospitals Leuven, Kapucijnenvoer 33, 3000 Leuven, Belgium
[f] Biomechanics Research Unit GIGA-R In Silico Medicine, Université de Liege, Quartier Hôpital, Avenue de l'Hôpital 11, Liège, Belgium
[g] Biomechanics Section, KU Leuven, Celestijnenlaan 300C (2419), Leuven, Belgium
[h] Department of Dental Medicine, Karolinska Institutet, Stockholm, Sweden

ARTICLE INFO

Keywords:
Gelatin
Chitosan
Maleic anhydride
3D printing
Dental tissue
Dental pulp stem cells

ABSTRACT

Dentoalveolar tissue engineering is an emerging yet challenging field, considering the lack of suitable materials and difficulty to produce patient-specific hydrogel scaffolds. The present paper aims to produce a 3D printable and tuneable biomaterial by copolymerizing a synthesized water-soluble chitosan derivative called maleic anhydride grafted chitosan (MA-C) with gelatin using genipin, a natural crosslinking agent. Development and testing of this material for 3D printing, degradation, and swelling demonstrated the ability to fabricate scaffolds with controlled physical properties based on pre-determined designs. The MA-C-gelatin copolymer demonstrated excellent biocompatibility, which was verified by analyzing the viability, growth and proliferation of human dental pulp stem cells seeded on MA-C-gelatin constructs through live/dead, alamar blue and DNA quantification assays. Based on the present findings, the proposed material might be a suitable candidate for dentoalveolar tissue engineering, while further research is required to achieve this goal.

1. Introduction

Dentoalveolar tissue loss affects millions of people around the world undermining their quality of life, by impacting both oral function and facial esthetics (Kassebaum et al., 2014; Mack et al., 2005). The limited regenerative capacity of the dentoalveolar tissues (Khodakaram-Tafti et al., 2018) is currently approached by oral surgical procedures such as dental implants or even tooth autotransplantation. While these treatments have come a long way, associated challenges such as the inability of implant placement in paediatric patients, or donor shortage for autotransplantation (EzEldeen et al., 2019; Hanif et al., 2017) may give rise to a demand for regenerative procedures. Consequently, tissue engineering has been proposed to address alveolar ridge resorption, tooth loss, condylar resorption, and craniofacial defects more effectively (Abou Neel et al., 2014).

The choice of the scaffold material is of significant importance and a wide range of material classes have been suggested as scaffolds for engineering soft tissues, including natural and synthetic polymers, hydrogels or bioceramics (Min et al., 2015). In particular, hydrogels have gained special interest due to their high water content and resemblance of the natural extracellular matrix (ECM) (Lee & Kim, 2018). However, it is rather challenging to produce precisely shaped constructs using traditional techniques with hydrogels. Consequently, 3D printing has been introduced as a novel method enabling the production of pre-designed scaffolds using hydrogels in their native form, called biomaterial inks, without any further processing (Groll et al.,

* Corresponding author at: Surface and Interface Engineered Materials (SIEM), Campus Group T, KU Leuven, Andreas Vesaliusstraat 13, 3000 Leuven, Belgium.
E-mail addresses: mehdi.salaramoli@kuleuven.be (M. Salar Amoli), resmi.anand@list.lu (R. Anand), mostafa.ezeldeen@kuleuven.be (M. EzEldeen), pauloalexandre.amorim@kuleuven.be (P.A. Amorim), liesbet.geris@uliege.be (L. Geris), reinhilde.jacobs@kuleuven.be (R. Jacobs), veerle.bloemen@kuleuven.be (V. Bloemen).

https://doi.org/10.1016/j.carbpol.2022.119441
Received 13 May 2021; Received in revised form 7 March 2022; Accepted 30 March 2022
Available online 2 April 2022

2018).

Chitosan, a polysaccharide originated from chitin, can form hydrogels capable of interacting electrostatically with GAGs distributed in natural ECM and thus, supporting the activity of cell attachment molecules and cytokines (Ahmadi et al., 2015; Islam et al., 2020). Furthermore, it is known to have an excellent biocompatibility, biodegradability and to possess antimicrobial properties (Seo et al., 2021), making it a suitable candidate for tissue engineering strategies. However, the insolubility of chitosan in neutral pH is a major disadvantage limiting the use of its hydrogels in any application requiring direct contact of cells with the material (Demirtaş et al., 2017). To overcome this, an interesting approach would be to synthesize chitosan derivatives capable of being dissolved in neutral pH.

While there are many suggested strategies to synthesize water-soluble chitosan, including modification of chitosan with styrene groups, azido groups (Rickett et al., 2011), methacryloyl groups (Amsden et al., 2007) etc., modification of chitosan with carboxylic groups through reaction with maleic anhydride (MA) is of particular interest due to the fast and effective procedure resulting in a sufficiently water-soluble chitosan derivative (Fu & Xiao, 2017).

Furthermore, being biocompatible, non-immunogenic, and biodegradable (Unal et al., 2020), gelatin has been used in combination with chitosan-based materials in tissue engineering applications to enhance cellular attachment to the chitosan, in addition to augmenting its mechanical properties (Kumar et al., 2017). However, for material solutions to form stable hydrogels, crosslinking is needed. Genipin is a naturally derived crosslinker able to attach primary amine groups and thus, crosslink both chitosan and gelatin (Maiz-Fernández et al., 2020), in addition to chitosan derivatives where the primary amines are still available for reaction. It has shown to induce a relatively lower amount of toxicity to the cells compared to other crosslinkers such as glutaraldehyde (Kirchmajer et al., 2013). Additionally, genipin is known to promote odontoblastic differentiation in dental pulp stem cells (DPSCs) (Kwon et al., 2015). Furthermore, using genipin allows for control over the physical properties of the scaffolds such as degradability or swelling, through adjusting the crosslinking degree. As a result, genipin appears to be a suitable crosslinker for production of scaffolds aimed at dentoalveolar regeneration.

We hypothesize that synthesis of a water-soluble chitosan derivative, maleic anhydride grafted chitosan (MA-C), in which the primary amines are available for further reactions such as crosslinking, and copolymerizing that with gelatin using genipin could produce a printable, tuneable material for fabrication of hydrogel scaffolds for dentoalveolar regeneration, while avoiding the use of acetic acid usually required for incorporation of chitosan. The present study aimed to synthesize the MA-C, and combine it with gelatin and genipin to investigate its potential for 3D printing, and to perform several physical characterizations and in vitro biocompatibility tests to assess suitability of the material to act as a tissue engineering scaffold.

2. Experimental

2.1. Materials

Chitosan (molecular weight 190–310 kDa, deacetylation rate 75–85%), maleic anhydride (purity >99%), pyridine (anhydrous, 99.8%), absolute ethanol, methanol (100%), glacial acetic acid, citric acid, NaOH, ninhydrin, tin(II) chloride dihydrate, glycine, gelatin (from porcine skin, 240–270 g bloom) were obtained from Sigma Aldrich (Overijse, Belgium). Genipin and alamar blue reagents were obtained from Challenge Bioproducts Co., Ltd. (Taiwan), and Thermo Fisher Scientific (Brussels, Belgium), respectively.

2.2. Preparation of hydrogels

2.2.1. Synthesis of maleic anhydride grafted chitosan (MA-C)

MA-C was synthesized through a reported procedure (Fu & Xiao, 2017) with slight modifications. Briefly, 1 g chitosan was dissolved in 50 mL 80% (v/v) acetic acid, and was then mixed with 30 mL 100% methanol in a 250 mL two-neck round bottom flask under stirring at room temperature. 1 g maleic anhydride was separately dissolved in 20 mL 100% methanol, and the solution was mixed with 1 mL pyridine by dropwise addition of pyridine in an ice water bath. The ice-cold solution was added to the chitosan dropwise and stirring was continued for 24 h at 65 °C. Excess ethanol was added to the reaction mixture to precipitate the MA-C, which was then recovered by centrifugation at rcf 155 for 10 min (Hettich Universal 32R) at room temperature. MA-C was added to excess water (approx. 750 mL) and dialyzed against deionized water using dialysis tubing with a 12 kDa molecular cut off for 5 days at room temperature to remove residual small molecules such as unreacted maleic anhydride and acetic acid. The solution was then freeze-dried to obtain the MA-C.

2.2.2. Preparation of genipin crosslinked MA-C/gelatin copolymers

Genipin component was dissolved in PBS (pH 7.4) in 5 different ratios of 0.5, 1, 1.5, 2 and 2.5 (w/w) % (with regards to the polymer content in the final combination) by heating to 60 °C followed by vortexing for 30s. Gel components were made separately by adding gelatin and MA-C to PBS (pH 7.4) and mixed by stirring at 60 °C for 24 h to yield final concentrations of 1.5%(w/v) gelatin and 1.5%(w/v) MA-C for the first set and 3%(w/v) gelatin and 1.5%(w/v) MA-C for the second set, achieving these concentrations after combination with genipin component. The two components (gel component and genipin) were mixed for 10 min, leading to 10 sets of combinations in total, and placed in a 37 °C water bath for 24 h to crosslink.

2.3. Physico-chemical characterization

2.3.1. Fourier transform infrared spectroscopy

MA-C and unmodified chitosan were freeze dried and grinded to prepare the samples. The FTIR-ATR spectra of the samples were recorded using a Bruker Vertex 70 FTIR spectrometer with a Diamond Attenuated Total Reflection (ATR) accessory in the wavelength range of 400–4000 cm^{-1}. The analysis was performed with a resolution of 2 cm^{-1} and an average of 32 scans on 3 samples for each condition.

2.3.2. Proton nuclear magnetic resonance (^1H NMR)

The structure of the synthesized MA-C was confirmed using ^1H NMR recorded on a Bruker Avance III HD/400, using D_2O as the solvent.

2.3.3. Measurement of the crosslinking degree

The degree of crosslinking was measured using the ninhydrin assay according to the protocols described by (Yan et al., 2010). A detailed protocol can be found in Appendix Section A.1.

2.3.4. Estimation of unreacted genipin

The amount of unreacted genipin in crosslinked samples was calculated by spectrophotometry. The detailed protocols for this analysis can be found in Appendix Section A.2.

2.4. 3D printing and physical characterizations of the scaffold

2.4.1. Evaluation of printing fidelity

The printing fidelity was evaluated by 3D printing the hydrogels using a 3DDiscovery bioprinter (RegenHU, Switzerland). The detailed protocol for this experiment is presented in Appendix Section A.3.

2.4.2. Evaluation of linear viscoelasticity of the material

The linear viscoelastic properties of the hybrid (physical and

chemical) and chemical hydrogels were measured via small-amplitude shear oscillatory measurements using an Anton Paar Physica MCR 501 rotational rheometer as in (Zuidema et al., 2014). Detailed protocols for these experiments are presented in Appendix Section A.4.

2.4.3. Evaluation of surface morphology

The surface morphology of the gels was evaluated by scanning electron microscopy. A detailed protocol for this analysis can be found in Appendix Section A.5.

2.4.4. Swelling and degradation studies

The rate of swelling and hydrolytic degradation for gel formulations of 3%(*w/v*) gelatin and 1.5%(w/v) chitosan-MA with 5 different genipin concentrations were measured according to reported procedures (Rosellini et al., 2009). Detailed protocols are presented in Appendix Section A.6.

2.5. Evaluation of cellular response

2.5.1. Isolation and culture of human dental pulp stem cells

Human dental pulp stem cells (hDPSCs) were isolated according to the explant method and expanded in culture as described previously (Hilkens et al., 2013). The process is described in details in Appendix Section A.7.

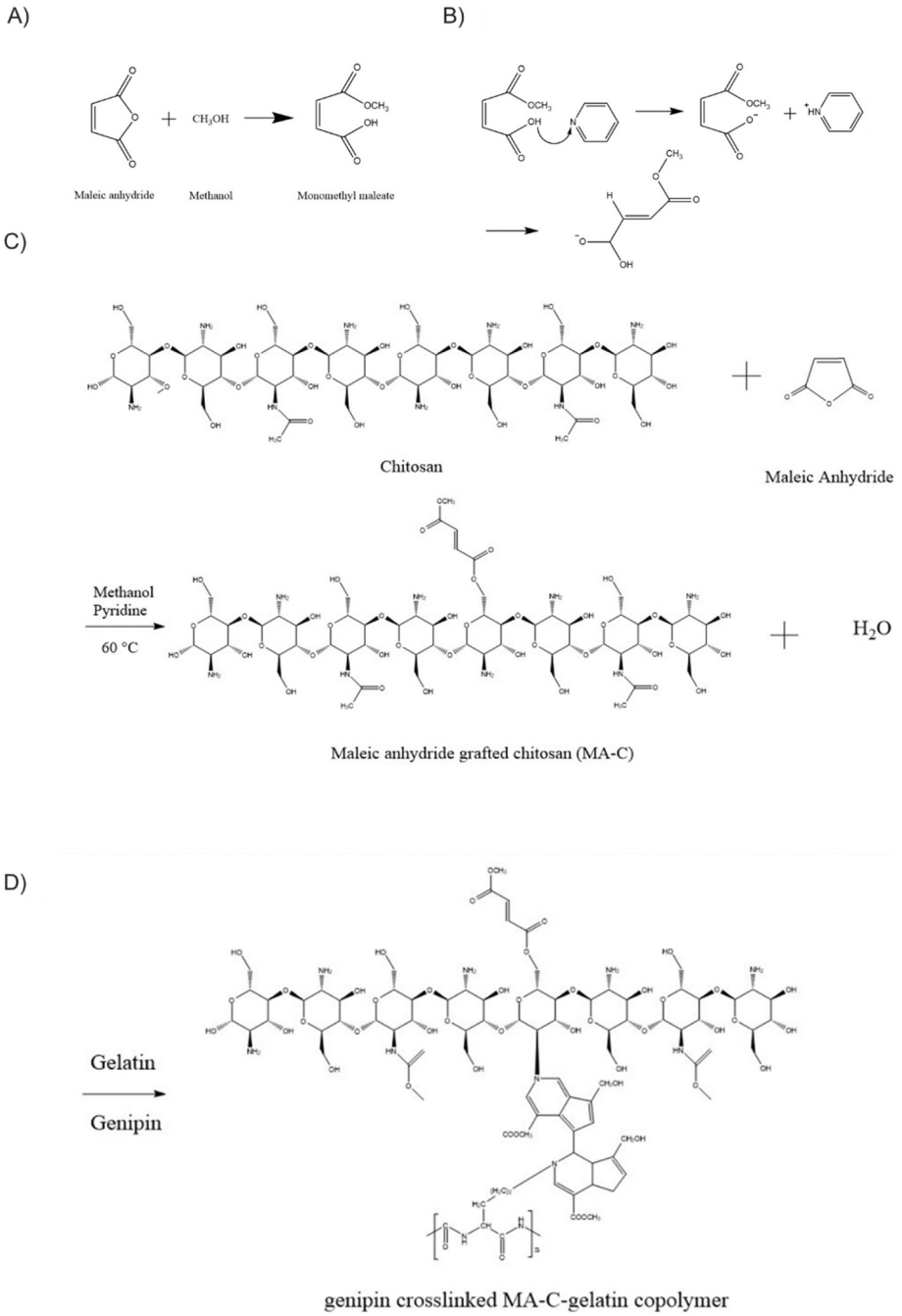

Scheme 1. Schematic representation showing the synthesis of maleic anhydride grafted chitosan, and copolymerization with gelatin through crosslinking with genipin. A) maleic anhydride reaction with methanol B) reaction of monomethyl maleate with pyridine C) overall reaction of MA-C synthesis D) synthesis of genipin crosslinked MA-C-gelatin copolymer.

2.5.2. Evaluation of cell viability through live/dead assay

The viability of dental pulp stem cells seeded on hydrogel scaffolds was evaluated by live/dead staining (Live/Dead viability cytotoxicity kit, Invitrogen, Thermofisher Scientific). The detailed protocol is presented in Appendix Section A.8.

2.5.3. Alamar blue assay

Alamar blue assay was performed on DPSCs seeded on the scaffolds according to manufacturers protocols. The detailed protocol for the assay is presented in Appendix Section A.9.

2.5.4. DNA quantification

DNA quantification was performed on DPSCs seeded on the hydrogel scaffolds by using Quant-iT dsDNA Assay Kit (Thermofisher Scientific, Belgium). Detailed protocols for the assay can be found in Appendix Section A.10.

2.6. Statistical analysis

All experiments in all sections were performed in three independent replicates ($n = 3$). Two-way ANOVA and Tukey's multiple comparisons test were performed using GraphPad Prism (version 8.0.0 for Windows, GraphPad Software, San Diego, California USA, www.graphpad.com) to

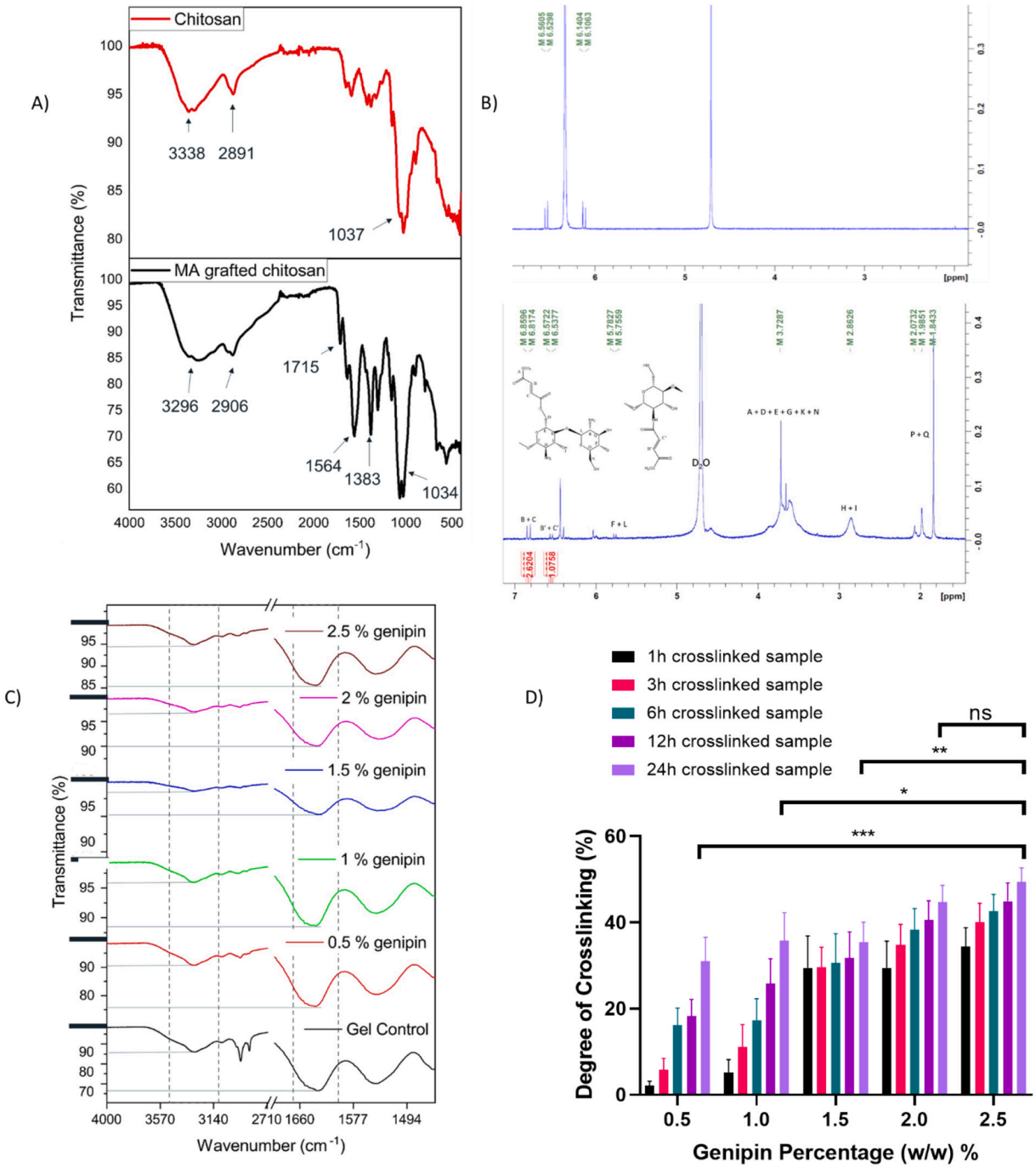

Fig. 1. A) FTIR spectra of chitosan (top) and synthesized MA-C (bottom). B) ^{1}H NMR spectrum of maleic anhydride (top) and MA-C (bottom) in D2O, C) confirmation of crosslinking through FTIR analysis, the area between dashed lines represent peaks corresponding to primary amine groups. D) Measurement of crosslinking degree through ninhydrin assay.

analyse differences with regards to time and genipin concentration. Graphs demonstrate mean ± standard deviation.

3. Results and discussion

3.1. Synthesis of MA-C

The structure of chitosan (Scheme 1.C), introduces a significant chance for formation of hydrogen bonds within the molecule structure, leading to a semi-crystalline structure that is not soluble in neutral pH (Qin et al., 2006). At pH lower than 6.5, the amino groups in the structure get protonated leading to a weak repulsion force enabling the solubility. However, a low pH is considered a major disadvantage for biological purposes. Consequently, introducing hydrophilic groups in the structure is required leading to increased solubility of chitosan in neutral pH.

For this purpose, an esterification reaction was performed between the chitosan and maleic anhydride. Firstly, maleic anhydride was dissolved in methanol, producing monomethyl maleate in a rapid, irreversible reaction (Induri et al., 2010) (Scheme 1.A).

Further reaction of monomethyl maleate with methanol will yield dimethyl maleate. However, that reaction is very slow and usually requires catalysers such as zeolite. At this step, pyridine is added to the reaction mixture to generate the functional groups required for reaction with the chitosan. Through the reaction of monomethyl maleate with pyridine (Scheme 1.B), it undergoes an isomerization turning into monomethyl fumarate, a more reactive form that may then react with chitosan (Karaman et al., 2013). As appears in Scheme 1.C, monomethyl fumarate produced in the second step reacts mainly with hydroxyl groups on chitosan backbone through an esterification reaction. The presence of ester groups leads to increased polarity of the chitosan, in addition to decreased intramolecular hydrogen bonds, leading to an increased solubility in neutral pH. The copolymer resulting from genipin crosslinking of MA-C and gelatin is demonstrated in Scheme 1.D.

3.2. Physico-chemical characterization

3.2.1. Fourier transform infrared spectroscopy

The FTIR analysis (Fig. 1.A) shows peaks appearing at 3000–3629, 2826–2987, 1715, 1564, 1383 and 959–1118 cm^{-1} corresponding to O—H/N—H, =C—H, C=O, C=C, C—N and C—O groups, the characteristic peaks aimed for. In particular, C=C peak observed at 1564 cm^{-1} demonstrates the success of modification considering these groups are only present on maleic anhydride and not on the chitosan backbone (Gopal Reddi et al., 2017; Lavanya et al., 2017), as shown in scheme 1.C. Further confirmation of the synthesis was performed using ^{1}H NMR, as represented in Fig. 1.B. The ^{1}H NMR peaks appearing at 6.5 ppm and 6.8 ppm represent alkene groups present on maleic anhydride confirming the grafting of maleic anhydride on the chitosan backbone. The peak appearing at 6.8 ppm represents the alkene close to the ester group, and the peak appearing at 6.5 represents the alkene group close to the amine group. Considering that the peak at 6.8 ppm is significantly larger than the one at 6.5, it can be concluded that the modification has mostly taken place on the hydroxyl groups rather than the amine groups. Peak integration demonstrates 70.8% of modification to have taken place at the hydroxyl groups of the chitosan.

3.2.2. Measurement of the degree of crosslinking in MA-C-gelatin copolymer

Firstly, a confirmation of crosslinking was obtained using FTIR analysis, as indicated in Fig. 1.C. The control material represents non crosslinked MA-C and gelatin combination. The wide peak of 3400–3600 cm^{-1} represents an overlap of primary amine groups and hydroxyl groups. A reduction observed in the intensity of primary amine peaks in this range, mainly in samples crosslinked with more than 1% (w/w) genipin, is a signal of efficient crosslinking. Similarly, the intensity of the N—H bending vibration of primary amines observed in the 1550–1650 cm^{-1} range is reduced significantly in the crosslinked samples, due to genipin reacting with primary amine groups (Cui et al., 2014). Moreover, a very slight increase in the ratio of C=O/N—H peaks at the wavelengths of 1700 cm^{-1} and 1400 cm^{-1}, observed in the peaks, is mentioned to be a hallmark of genipin crosslinking (Y. Zhang et al., 2016).

Furthermore, the ninhydrin assay provides information on the percentage of free amine groups in the samples, thus, representing an estimate of the percentage of amine groups involved in crosslinking reaction. As indicated in Fig. 1.D, higher crosslinking times leads to higher crosslinking degrees, however, the rate of increase in crosslinking degree is reduced as time goes on, represented by the slope of the curves in the graph, due to more genipin being spent in the reaction. The ANOVA model shows a significant effect for both the effects of time and genipin concentration. Consequently, 2.5 wt% genipin leads to crosslinking degrees which are significantly higher than 0.5 wt% ($p \leq 0.001$), 1 wt% ($p \leq 0.05$) and 1.5 wt% ($p \leq 0.01$) genipin after 24 h of crosslinking. Considering the synthesis procedure described mainly engage the hydroxyl group on the chitosan backbone leaving the majority of the amine groups free to react with genipin, the crosslinking degree was expected to be in the same range observed with similar materials. This is the case considering genipin crosslinked chitosan/gelatin films have been reported to result in 65% crosslinking degree using 1.5% genipin (Koc & Altıncekic, 2020). Furthermore, the difference in crosslinking degree based on genipin concentration, can lead to a control over physical and mechanical properties of the scaffold through controlled crosslinking, assisting in production of tailor-made scaffolds for different applications. This method has been used previously to fabricate collagen-based scaffolds with controlled properties (Davidenko et al., 2015).

3.2.3. Estimation of unreacted genipin

Genipin is a crosslinker reacting with primary amine groups. Consequently, it is a favourable material for crosslinking of chitosan and gelatin. Being naturally derived, genipin has a lower cytotoxicity than other crosslinkers such as GPTMS ((3-Glycidyloxypropyl)trimethoxysilane) or glutaraldehyde (Sung et al., 1999). Still, concentrations of over 1 mg/mL are known to be toxic to most cell types. However, a concentration of around 100 μg/mL was determined in the literature to induce odontoblastic differentiation in DPSCs (Kwon et al., 2015). As a result, it is vital to determine the amount of unreacted genipin released from the scaffolds to ensure cytocompatibility of the scaffolds. ANOVA analysis shows a significant effect for both crosslinking time and genipin concentration on the amount of unreacted genipin ($p < 0.0001$). As demonstrated in Fig. 2, the amount of unreacted genipin released from scaffolds decreases significantly with an increase in crosslinking time, with the amount being close to 100 μg/mL after 24 h of crosslinking

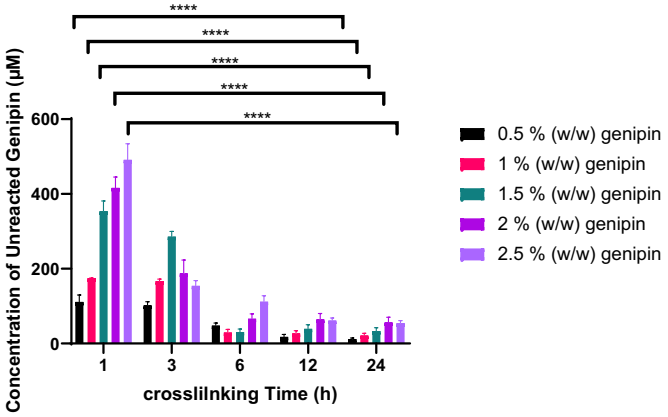

Fig. 2. The amount of unreacted genipin based on the crosslinking time.

(significantly different from 1 h crosslinking time, $p < 0.0001$), which would be the optimum amount shown not to induce any toxicity (Kwon et al., 2015).

Furthermore, Tukey's multiple comparisons show a significant difference between samples crosslinked with 0.5 wt% genipin with those crosslinked with 2 wt% and 2.5 wt% genipin ($p \leq 0.05$) after 24 h, and with smaller variabilities in genipin concentration there is no significant differences. However, the remaining genipin is in the non-toxic region for all concentrations.

3.3. 3D printing and physical characterizations of the scaffold

3.3.1. Evaluation of printing fidelity

To analyse the possibility of 3D printing scaffolds based on predetermined designs using the proposed hydrogels, the printability of the materials was evaluated. Different combinations of gelatin, MA-C and genipin have been used for this purpose, and constructs printed with them can be seen in Fig. 3.

Fig. 3 demonstrates the hydrogels containing 1.5%(*w/v*) MA-C and 3%(w/v) gelatin yield much more accurate printed constructs representing the design, which was expected as gelatin is known to augment the mechanical properties of chitosan and thus, its ability to maintain its 3D structure (Benbettaïeb et al., 2014). This was also confirmed by measuring the strand width to evaluate uniformity of the diameter of the printed strands at different locations on the sample. As shown in Table 1, these measurements demonstrate that the variability in strand width is not significant, confirming uniformity across the printed constructs.

3.3.2. Evaluation of linear viscoelasticity

Due to the viscoelastic character of the blend hydrogels, oscillatory shear measurements provide a representative description of their mechanical behavior at small deformations, in which the linear viscoelasticity theory is held. Therefore, the mechanical spectra of the gelatin/chitosan MA crosslinked with low (0.5 wt%) and high (2.5 wt%) genipin concentrations were obtained via frequency sweep tests, as presented in Fig. 4. For the determination of the linear viscoelastic envelope (LVE), please refer to Fig. A.2.

In this type of experiment, the elastic and viscous responses given by the storage (G′) and loss (G″) moduli are monitored against the angular frequency of the applied sinusoidal oscillation. The storage modulus is a measure of the stored energy per oscillation cycle whereas the loss modulus (G″) is a measure of dissipated energy as heat per cycle of sinusoidal deformation (Ferry, 1970). Thus, the mechanical spectra allow for the observation of the time-dependent mechanical behavior of the materials, within a relatively broad range of observation times.

Table 1
Measurement of strand width in samples containing 1.5%(w/v) MA-C, 3%(w/v) gelatin and varying amounts of genipin. Line numbers correspond to different lines within a single printed shape, the lines are presented in the schematic in Fig. 3.A.

MA-C 1.5% Gelatin 3%	0.5 wt% genipin	1 wt% genipin	1.5 wt% genipin	2 wt% genipin	2.5 wt% genipin
Line 1 (mm)	1.6 ± 0.1	1.6 ± 0.3	1.7 ± 0.1	1.8 ± 0.1	1.6 ± 0.1
Line 2 (mm)	1.7 ± 0.1	1.7 ± 0.2	1.7 ± 0.2	1.7 ± 0.1	1.6 ± 0.1
Line 3 (mm)	1.7 ± 0.2	1.8 ± 0.4	1.7 ± 0.3	1.8 ± 0.2	1.7 ± 0.1

In all the scenarios tested, the materials present higher magnitudes of G′ over G″ within a range of four orders of magnitude of angular frequencies. This result was expected as it reveals that conformational changes at both short and long length scales are hindered by the presence of gel networks. The strong frequency-independency of the moduli, as a consequence of their supramolecular structures, is a remarkable characteristic of the mechanical spectra of gels, such as the materials herein studied.

The mechanical spectra of both the hybrid and chemical gels revealed the existence of imperfect polymer networks due to the frequency dependency of their loss moduli. However, no evidence of terminal behavior (G′ = G″) was seen. In all the conditions, their mechanical spectra are situated in the rubbery plateau. The frequency dependency of the loss modulus suggests the presence of network defects such as dangling structures, branching and sol phase. This is probably attributed to the crosslinking conditions of the hydrogels applied in this work.

At 37 °C, the gelatin chains are transitioning from random coil to worm-like conformation as their sol-gel temperature is being approached (Ross-Murphy, 1992). The presence of these random coils at

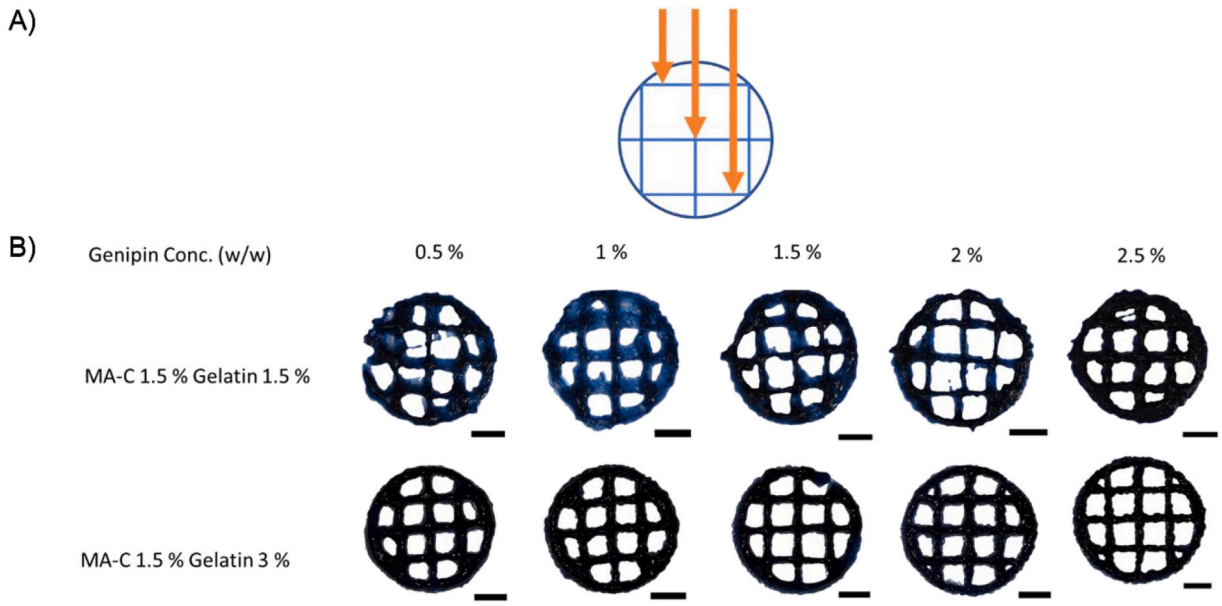

Fig. 3. A) computer aided design, arrows represent lines used for measurements in Table 1 B) Printability of different gelatin, chitosan MA and genipin concentrations. 5 layer constructs, scale bar 5 mm.

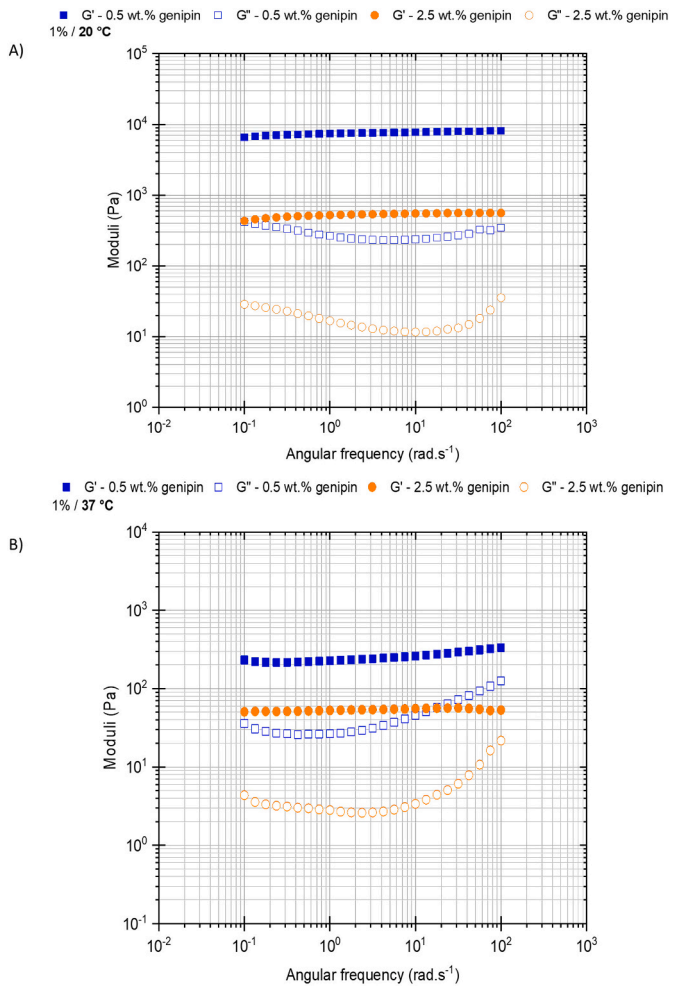

Fig. 4. Mechanical spectra of gelatin/chitosan MA with low (0.5 wt%) and high (2.5 wt%) genipin contents. (A) hybrid hydrogel blends at the 3D printing temperature of 20 °C and (B) the chemical hydrogels at the physiological temperature of 37 °C.

37 °C favor the reaction of genipin molecules with the amine groups present in the lysine residues of the gelatin and chitosan chains, as those are more exposed at such molecular conformation (Butler et al., 2003). The existence of an imperfect gel network is convenient in terms of both the 3D printing process and cell proliferation. An extremely elastically dominated microstructure would result in filament rupture and an unfavorable environment for cell attachment and, thus, poorer viability and proliferation (Amorim et al., 2021).

Interestingly, the moduli of the hybrid hydrogels formulations with 2.5 w/w% and 0.5 w/w% genipin are shifted approximately one order of magnitude apart at 20 °C. This result suggests that the high (2.5 wt%) genipin concentration has a stronger influence in inhibiting the physical gelation of gelatin at temperatures below its sol-gel transition, such as 20 °C. Thus, the benefits of applying this blend in 3D printing are guaranteed.

On the other hand, the observed difference in moduli at 37 °C is likely related to the aforementioned chemical gelation conditions used in this work. Chemical gelation of gelatin and chitosan in presence of genipin is reported to be substantially more effective at slightly higher temperatures (Cui et al., 2014). However, the lower storage modulus seen for the 2.5 wt% could be associated with polymerization of genipin molecules as previously reported (Butler et al., 2003), resulting in longer crosslinks and, thus, a weaker gel due to excess of genipin. Therefore, we estimate the spatial correlation length of the materials from rheological measurements, which is known as the size of the elastic blob. This spatial correlation length gives us an estimate size of the elastic active network chains. The size of the elastic blob (ξel) is given by Eqs. (1) and (2) (Tsuji et al., 2018):

$$G' = \rho_{el} k_B T \tag{1}$$

$$\xi_{el} = (\rho_{el})^{-\frac{1}{3}} \tag{2}$$

Taking G′ at 0.1 rad.s^{-1} at 37 °C so that G′ ≈ 200 Pa and 50 Pa for the 0.5 and 2.5 w/w%, geninipin concentration formulations respectively, the size of the elastic blob of the blend hydrogels can be estimated from Eqs. (1) and (2), where k_B is the Boltzmann constant, T is the absolute temperature and ρel is the density of the elastic blob.

As hypothesized before, the size of the elastic blobs of the chemical 2.5 w/w% genipin crosslinked hydrogel is approximately 30% greater than the 0.5 w/w% counterpart, suggesting interpolymerization of genipin molecules.

3.3.3. Swelling and degradation studies

Hydrogel swelling is an indicator of hydrogels water content, thus, its measurement can be crucial in anticipating cellular response and mechanical behavior of the scaffold.

Fig. 5. A shows that the swelling ratio ranges from 6 to 8 times depending on the crosslinker concentration. It is also noteworthy that the main water uptake takes place within 24 h of scaffold placement in PBS due to the rapid penetration of the PBS into the material structure (Ganji et al., 2010). Observed swelling is higher compared to other chitosan-based materials, with a combination of chitosan, gelatin and bioglass resulting in swelling of approximately 1.6 times (Maji et al., 2016) and a combination of chitosan and gelatin as a 2D film resulting in swelling ratio of approximately 3.5 in pH 7.4 (Ling et al., 2004), This higher swelling observed is attributed to increased hydrophilicity of the synthesized water-soluble chitosan derivative. Two-way ANOVA showed significant effects of both time and genipin concentration on the swelling. Further multiple comparisons show significant differences in the swelling of all different comparisons of genipin concentrations ($p \leq 0.0001$), except for 0.5 versus 1 wt% and 1.5 versus 2 wt%.

Moreover, the degradation rate is of significant importance in tissue engineering allowing for natural tissue to regenerate and replace the scaffold. The rate of hydrolytic degradation of the printed scaffolds (Fig. 5.B) demonstrates the maximum degradation within 14 days of immersion in PBS to be approximately 40%, and ANOVA analysis demonstrates the significant effect of both factors on degradation. However, after 7 days, differences in genipin concentration leads to significant differences among degradation rates of the samples ($p \leq 0.01$), except for comparisons among samples crosslinked with 0.5 wt% versus 1 wt% and 1.5 wt% versus 2 wt%. While the maleic anhydride grafting mainly takes place on the hydroxyl groups of the chitosan backbone, leaving majority of the amine groups free for reaction with genipin, the increased hydrophilicity in the synthesized material could potentially lead to increased hydrolytic degradation rates for the scaffolds. This is represented by degradation of similar materials being in the range of 25 to 30% (Fischetti et al., 2020). These results suggest the crosslinker concentration as an effective tool to control the physical behaviours of the scaffolds by controlling the crosslinking degree.

3.3.4. Scanning electron microscopy

The SEM images of the cross-section of the scaffolds prepared with 0.5 wt% and 2.5 wt% genipin are presented in Fig. 6. As the hydrogels in this study are used in the wet state, these images can offer insights into the effect of the crosslinker concentration on the pore size of the hydrogels. Both samples appear in SEM images to have a large degree of porosity, confirming the swelling finding regarding the high water content. It appears that gels crosslinked with 0.5 wt% genipin have a larger pore diameter of average 86.3 ± 8.1 μm, while pore diameter in gels crosslinked with 2.5 wt% genipin is in the range of 63.6 ± 6.8 μm.

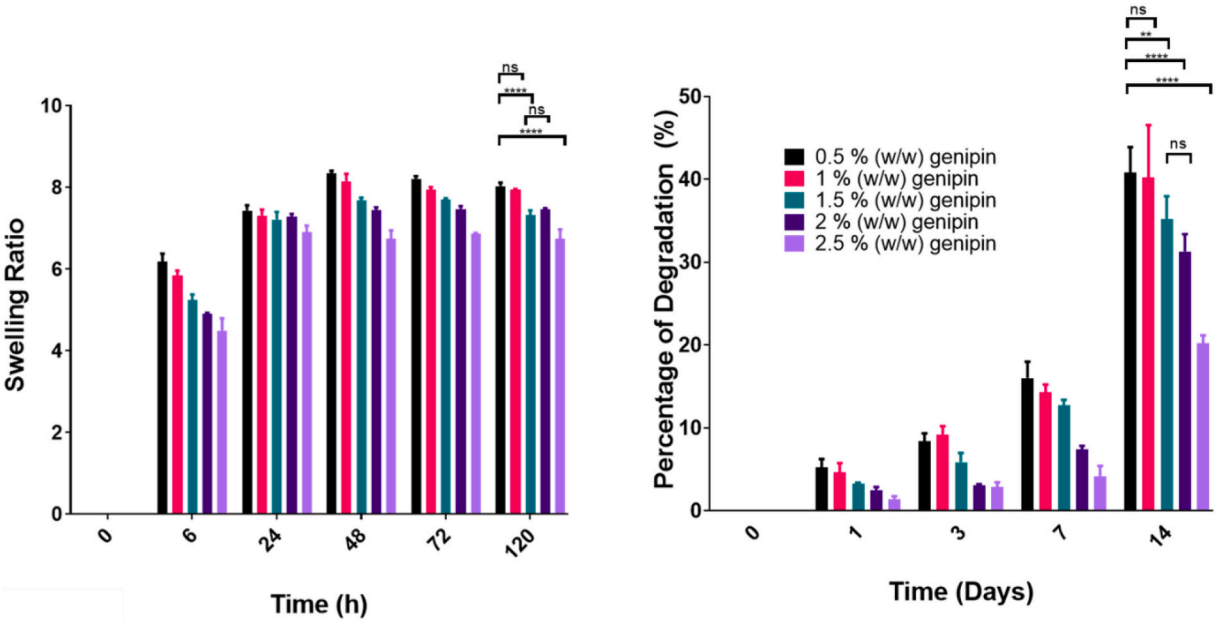

Fig. 5. A) swelling rate of printed hydrogel scaffolds B) Hydrolytic degradation rate of printed hydrogel scaffolds.

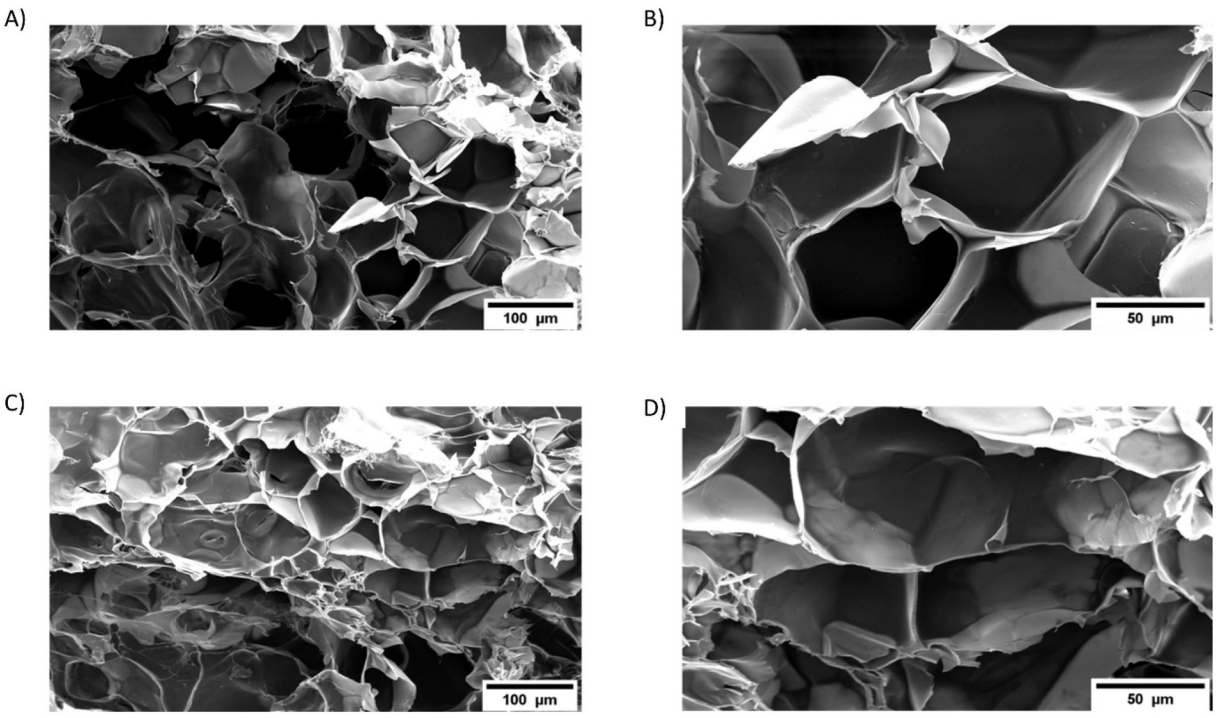

Fig. 6. Scanning electron microscopy of the cross-section of 3D printed hydrogels A) 0.5 wt% genipin, 200× B) 0.5 wt% genipin 500× C) 2.5 wt% genipin 200× D) 2.5 wt% genipin 500×.

This pore size is in the range observed with other chitosan-based materials such as chitosan/collagen where a pore size of 50–150 μm was observed (Yan et al., 2010) or chitosan/gelatin scaffolds were a pore size of approximately 102 μm was obtained (Mao et al., 2003).

3.4. Cellular responses

3.4.1. Live/Dead assay

A critical property any tissue engineering scaffold must possess is biocompatibility, considered in this context as both lack of any toxicity and presence of cell adhesion cues. The possible toxicity of the material on the cells can be viewed using live/dead staining. In this section, only gels containing 2.5 wt% and 0.5 wt% genipin were evaluated, representing the extreme concentrations. Results of the live/dead assay can be seen in Fig. 7. A qualitative analysis of the pictures in all timepoints demonstrates that there is no visible difference in cell viability among cells cultured on the scaffolds and control samples with cells cultured on the well plates. This highlights for the first time that the MA-C does not have any adverse effect on the viability of hDPSCs, and the remaining genipin is non-toxic as expected (Kwon et al., 2015). Additionally, cells

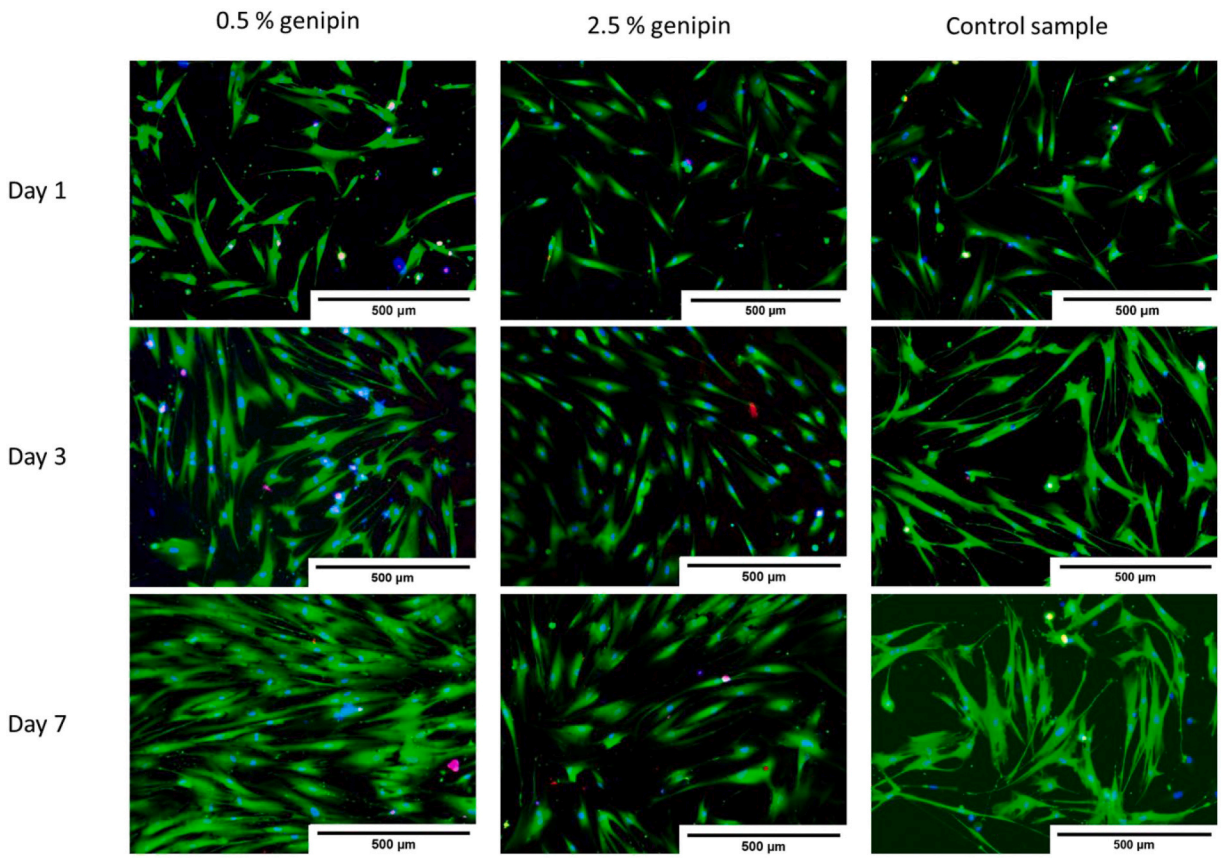

Fig. 7. Viability of cells seeded on gels with different genipin concentrations, green represents live cells, red represents dead cells and blue represents cell nucleus.

demonstrate the stretched form showing their adherence to the gel and exhibiting efficiency of the proposed hydrogel in supporting cell attachment and spreading.

3.4.2. *Alamar blue assay*

Alamar blue assay (Fig. 8.A) was performed to assess metabolic activity of the cells. ANOVA analysis shows a significant effect for both time and genipin concentration on the metabolic activity of the cells. After one day of culture, the sample with 2.5 wt% genipin shows a significantly higher metabolic activity compared to the sample with 0.5 wt% genipin, and the difference of 0.5 wt% with control samples are significant ($p < 0.05$).

However, on day 3, the readings for all samples are significantly different from each other. After 7 days of culture, only the difference of the metabolic activity of cells cultured on scaffold crosslinked with 0.5 wt% genipin is significantly different than the control ($p \leq 0.05$). These results confirm the viability data as the cells cultured on MA-C-gelatin scaffolds maintain their metabolic activity. These observations are in-line with other studies using genipin crosslinked chitosan where, similar to our obtained results, there is no vast difference in metabolic activity with regards to the genipin concentration after 7 days of culture (Dimida et al., 2017). Furthermore, an overall reduction in alamar blue readings at day 7 could be observed. While further in-depth analysis of the biological processes in the future could determine the exact cause of this behavior, it can be attributed to contact inhibition resulting from high proliferation of the cells, which can lead to reduced metabolic

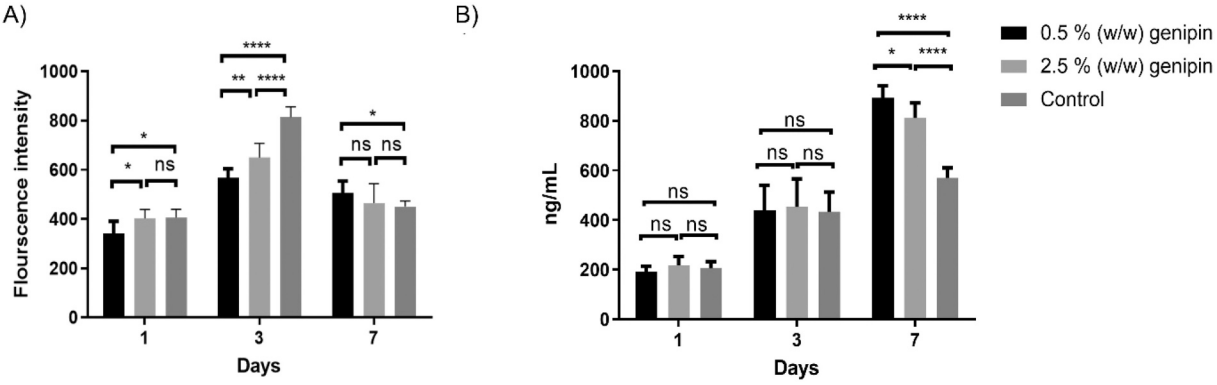

Fig. 8. A) Alamar blue readings analysed at day 1, 3, and 7 B) DNA concentration relative to hydrogel volume, analysed at day 1, 3, and 7. Results shown as average ± standard deviation, ($n = 3$), ns shows no significant difference, * stands for difference ($p < 0.05$), ** stands for difference ($p < 0.01$), and **** stands for difference ($p < 0.0001$).

activity (Gallorini et al., 2021; Ng et al., 2005).

3.4.3. DNA quantification

A DNA quantification assay was performed to further investigate the effects on cell viability (Fig. 8.B). The DNA content almost tripled within 7 days. Similar to alamar blue assay, ANOVA analysis demonstrates both time and genipin concentration to have a significant effect on the DNA content. Additionally, while after 1 and 3 days of culture the difference of the DNA content in samples is not significantly different from the control group, at 7 days, DNA content is significantly higher in scaffolds compared to the control group ($p \leq 0.0001$). This effect can be attributed to the presence of a 3D environment including gelatin, providing a more favourable space for cell proliferation, an effect known to occur within 3D collagen scaffolds (Jensen & Teng, 2020). Similar behavior has been observed in other studies incorporating gelatin and chitosan where a DNA content larger than the 2D control was considered as a sign of suitability of the scaffold for tissue engineering applications (Gautam et al., 2014). Taken together, these results confirm the absence of any toxicity, confirming the pattern obtained through live/dead analysis.

4. Conclusion

Through synthesis of maleic anhydride grafted chitosan (MA-C), a water-soluble derivative of chitosan was obtained which could be copolymerised with gelatin in the presence of genipin to yield a 3D printable hydrogel, capable of forming tissue engineering scaffolds. Being used for the first time as a tissue engineering scaffold, it was shown that neither the synthesized material, nor any of the crosslinker concentrations used, were toxic to hDPSCs. Moreover, as a range of physical properties might be needed for tissue engineering in the dentoalveolar region, it was demonstrated using different concentrations of genipin as crosslinker, physical properties of the scaffold can be adequately tuned. Consequently, it can be concluded that the proposed material could be considered as a candidate for production of scaffolds for regeneration of soft tissues in the alveolar region. As a next step, in-depth biological validations are required to investigate cell differentiation and matrix formation in these novel scaffolds.

CRediT authorship contribution statement

Mehdi Salar Amoli: Conceptualization, Methodology, Writing – original draft, Investigation, Data curation. **Resmi Anand:** Conceptualization, Methodology, Writing – review & editing, Investigation. **Mostafa EzEldeen:** Conceptualization, Methodology, Writing – review & editing. **Paulo Alexandre Amorim:** Methodology, Writing – review & editing, Investigation. **Liesbet Geris:** Writing – review & editing, Funding acquisition. **Reinhilde Jacobs:** Conceptualization, Resources, Writing – review & editing, Supervision, Funding acquisition. **Veerle Bloemen:** Conceptualization, Resources, Methodology, Writing – review & editing, Supervision, Project administration, Funding acquisition.

Declaration of competing interest

The authors declare no conflict of interests.

Acknowledgements

Supported by the Research Council of KU Leuven grant number (C24/18/068), and the European Research Council (ERC) under the European Union's Horizon 2020 research and innovation programme (ERC CoG 772418). RA acknowledges DST INSPIRE Faculty award (DST/INSPIRE/04/2016/000482).

Appendix A. Supplementary data

Supplementary data to this article can be found online at https://doi.org/10.1016/j.carbpol.2022.119441.

References

Abou Neel, E. A., Chrzanowski, W., Salih, V. M., Kim, H.-W., & Knowles, J. C. (2014). Tissue engineering in dentistry. *Journal of Dentistry, 42*(8), 915–928. https://doi.org/10.1016/J.JDENT.2014.05.008

Ahmadi, F., Oveisi, Z., Samani, S. M., & Amoozgar, Z. (2015). Chitosan based hydrogels: Characteristics and pharmaceutical applications. *Research in Pharmaceutical Sciences, 10*(1), 1–16.

Amorim, P. A., d'Ávila, M. A., Anand, R., Moldenaers, P., Van Puyvelde, P., & Bloemen, V. (2021). Insights on shear rheology of inks for extrusion-based 3D bioprinting. *Bioprinting, 22*, Article e00129. https://doi.org/10.1016/j.bprint.2021.e00129

Amsden, B. G., Sukarto, A., Knight, D. K., & Shapka, S. N. (2007). Methacrylated glycol chitosan as a photopolymerizable biomaterial. *Biomacromolecules, 8*(12), 3758–3766. https://doi.org/10.1021/bm700691e

Benbettaïeb, N., Kurek, M., Bornaz, S., & Debeaufort, F. (2014). Barrier, structural and mechanical properties of bovine gelatin-chitosan blend films related to biopolymer interactions. *Journal of the Science of Food and Agriculture, 94*(12), 2409–2419. https://doi.org/10.1002/jsfa.6570

Butler, M. F., Ng, Y.-F., & Pudney, P. D. A. (2003). Mechanism and kinetics of the crosslinking reaction between biopolymers containing primary amine groups and genipin. *Journal of Polymer Science Part A: Polymer Chemistry, 41*(24), 3941–3953. https://doi.org/10.1002/pola.10960

Cui, L., Jia, J., Guo, Y., Liu, Y., & Zhu, P. (2014). Preparation and characterization of IPN hydrogels composed of chitosan and gelatin cross-linked by genipin. *Carbohydrate Polymers, 99*, 31–38. https://doi.org/10.1016/j.carbpol.2013.08.048

Davidenko, N., Schuster, C. F., Bax, D. V., Raynal, N., Farndale, R. W., Best, S. M., & Cameron, R. E. (2015). Control of crosslinking for tailoring collagen-based scaffolds stability and mechanics. *Acta Biomaterialia, 25*, 131–142. https://doi.org/10.1016/j.actbio.2015.07.034

Demirtaş, T. T., Irmak, G., & Gümüşderelioğlu, M. (2017). A bioprintable form of chitosan hydrogel for bone tissue engineering. *Biofabrication, 9*(3), 35003. https://doi.org/10.1088/1758-5090/aa7b1d

Dimida, S., Barca, A., Cancelli, N., De Benedictis, V., Raucci, M. G., & Demitri, C. (2017). Effects of genipin concentration on cross-linked chitosan scaffolds for bone tissue engineering: Structural characterization and evidence of biocompatibility features. *International Journal of Polymer Science, 2017*, Article 8410750. https://doi.org/10.1155/2017/8410750

EzEldeen, M., Wyatt, J., Al-Rimawi, A., Coucke, W., Shaheen, E., Lambrichts, I. Jacobs, R., … (2019). Use of CBCT guidance for tooth autotransplantation in children. *Journal of Dental Research, 98*(4), 406–413. https://doi.org/10.1177/0022034519828701

Ferry, J. D. (1970). Viscoelastic properties of polymers / [by] John D. Ferry. Retrieved from http://www.loc.gov/catdir/enhancements/fy0608/76093301-t.html.

Fischetti, T., Celikkin, N., Contessi Negrini, N., Farè, S., & Swieszkowski, W. (2020). Tripolyphosphate-crosslinked chitosan/gelatin biocomposite ink for 3D printing of uniaxial scaffolds. Retrieved from *Frontiers in Bioengineering and Biotechnology, 8*, 400 https://www.frontiersin.org/article/10.3389/fbioe.2020.00400.

Fu, Y., & Xiao, C. (2017). A facile physical approach to make chitosan soluble in acid-free water. *International Journal of Biological Macromolecules, 103*, 575–580. https://doi.org/10.1016/j.ijbiomac.2017.05.066

Gallorini, M., Zara, S., Ricci, A., Mangano, F. G., Cataldi, A., & Mangano, C. (2021). The open cell form of 3D-printed titanium improves osteconductive properties and adhesion behavior of dental pulp stem cells. *Materials, 14*. https://doi.org/10.3390/ma14185308

Ganji, F., Vasheghani Farahani, S., & Vasheghani-Farahani, E. (2010). Theoretical description of hydrogel swelling: A review. *Iranian Polymer Journal, 19*, 375–398.

Gautam, S., Chou, C.-F., Dinda, A. K., Potdar, P. D., & Mishra, N. C. (2014). Fabrication and characterization of PCL/gelatin/chitosan ternary nanofibrous composite scaffold for tissue engineering applications. *Journal of Materials Science, 49*(3), 1076–1089. https://doi.org/10.1007/s10853-013-7785-8

Gopal Reddi, M. R., Gomathi, T., Saranya, M., & Sudha, P. N. (2017). Adsorption and kinetic studies on the removal of chromium and copper onto chitosan-g-maliec anhydride-g-ethylene dimethacrylate. *International Journal of Biological Macromolecules, 104*, 1578–1585. https://doi.org/10.1016/j.ijbiomac.2017.01.142

Groll, J., Burdick, J. A., Cho, D.-W., Derby, B., Gelinsky, M., Heilshorn, S. C. Woodfield, T. B. F., … (2018). A definition of bioinks and their distinction from biomaterial inks. *Biofabrication, 11*(1), 13001. https://doi.org/10.1088/1758-5090/aaec52

Hanif, A., Qureshi, S., Sheikh, Z., & Rashid, H. (2017). Complications in implant dentistry. *European Journal of Dentistry, 11*(1), 135–140. https://doi.org/10.4103/ejd.ejd_340_16

Hilkens, P., Gervois, P., Fanton, Y., Vanormelingen, J., Martens, W., Struys, T. Bronckaers, A., … (2013). Effect of isolation methodology on stem cell properties and multilineage differentiation potential of human dental pulp stem cells. *Cell and Tissue Research, 353*(1), 65–78. https://doi.org/10.1007/s00441-013-1630-x

Induri, S., Sengupta, S., & Basu, J. K. (2010). A kinetic approach to the esterification of maleic anhydride with methanol on H-Y zeolite. *Journal of Industrial and Engineering Chemistry, 16*(3), 467–473. https://doi.org/10.1016/j.jiec.2010.01.053

Islam, M. M., Shahruzzaman, M., Biswas, S., Nurus Sakib, M., & Rashid, T. U. (2020). Chitosan based bioactive materials in tissue engineering applications-a review. *Bioactive Materials, 5*(1), 164–183. https://doi.org/10.1016/j.bioactmat.2020.01.012

Jensen, C., & Teng, Y. (2020). Is it time to start transitioning from 2D to 3D cell culture?. Retrieved from *Frontiers in Molecular Biosciences, 7*, 33 https://www.frontiersin.org/article/10.3389/fmolb.2020.00033.

Karaman, R., Dokmak, G., Bader, M., Hallak, H., Khamis, M., Scrano, L., & Bufo, S. A. (2013). Prodrugs of fumarate esters for the treatment of psoriasis and multiple sclerosis—a computational approach. *Journal of Molecular Modeling, 19*(1), 439–452. https://doi.org/10.1007/s00894-012-1554-5

Kassebaum, N. J., Bernabé, E., Dahiya, M., Bhandari, B., Murray, C. J. L., & Marcenes, W. (2014). Global burden of severe periodontitis in 1990–2010: A systematic review and meta-regression. *Journal of Dental Research, 93*(11), 1045–1053. https://doi.org/10.1177/0022034514552491

Khodakaram-Tafti, A., Mehrabani, D., Shaterzadeh-Yazdi, H., Zamiri, B., & Omidi, M. (2018). Tissue engineering in maxillary bone defects. Retrieved from *World Journal of Plastic Surgery, 7*(1), 3–11 https://pubmed.ncbi.nlm.nih.gov/29651386.

Kirchmajer, D. M., Watson, C. A., Ranson, M., & Panhuis, M.i.h. (2013). Gelapin, a degradable genipin cross-linked gelatin hydrogel. *RSC Advances, 3*(4), 1073–1081. https://doi.org/10.1039/C2RA22859A

Koc, F. E., & Altıncekic, T. G. (2020). Investigation of gelatin/chitosan as potential biodegradable polymer films on swelling behavior and methylene blue release kinetics. *Polymer Bulletin*. https://doi.org/10.1007/s00289-020-03280-7

Kumar, P., Dehiya, B. S., & Sindhu, A. (2017). Comparative study of chitosan and chitosan–gelatin scaffold for tissue engineering. *International Nano Letters, 7*(4), 285–290. https://doi.org/10.1007/s40089-017-0222-2

Kwon, Y.-S., Lim, E.-S., Kim, H.-M., Hwang, Y.-C., Lee, K.-W., & Min, K.-S. (2015). Genipin, a cross-linking agent, promotes odontogenic differentiation of human dental pulp cells. *Journal of Endodontics, 41*(4), 501–507. https://doi.org/10.1016/j.joen.2014.12.002

Lavanya, R., Gomathi, T., Vijayalakshmi, K., Saranya, M., Sudha, P. N., & Anil, S. (2017). Adsorptive removal of copper (II) and lead (II) using chitosan-g-maleic anhydride-g-methacrylic acid copolymer. *International Journal of Biological Macromolecules, 104*, 1495–1508. https://doi.org/10.1016/j.ijbiomac.2017.04.116

Lee, J.-H., & Kim, H.-W. (2018). Emerging properties of hydrogels in tissue engineering. *Journal of Tissue Engineering, 9*. https://doi.org/10.1177/2041731418768285, 2041731418768285.

Ling, X., Zu-yu, Y., Chao, Y., Hua-yue, Z., & Yu-min, D. (2004). Swelling studies of chitosan-gelatin films cross-linked by sulfate. *Wuhan University Journal of Natural Sciences, 9*(2), 247–251. https://doi.org/10.1007/BF02830611

Mack, F., Schwahn, C., Feine, J. S., Mundt, T., Bernhardt, O., John, U.Biffar, R., … (2005). The impact of tooth loss on general health related to quality of life among elderly Pomeranians: Results from the study of health in Pomerania (SHIP-O). *The International Journal of Prosthodontics, 18*(5), 414–419.

Maiz-Fernández, S., Guaresti, O., Pérez-Álvarez, L., Ruiz-Rubio, L., Gabilondo, N., Vilas-Vilela, J. L., & Lanceros-Mendez, S. (2020). β-Glycerol phosphate/genipin chitosan hydrogels: A comparative study of their properties and diclofenac delivery. *Carbohydrate Polymers, 248*, Article 116811. https://doi.org/10.1016/j.carbpol.2020.116811

Maji, K., Dasgupta, S., Pramanik, K., & Bissoyi, A. (2016). Preparation and evaluation of gelatin-chitosan-nanobioglass 3D porous scaffold for bone tissue engineering. *International Journal of Biomaterials, 2016*, 9825659. https://doi.org/10.1155/2016/9825659

Mao, J. S., Zhao, L. G., Yin, Y. J., & Yao, K. D. (2003). Structure and properties of bilayer chitosan–gelatin scaffolds. *Biomaterials, 24*(6), 1067–1074. https://doi.org/10.1016/S0142-9612(02)00442-8

Min, L. J., Edgar, T. Y. S., Zicheng, Z., & Yee, Y. W. (2015). *Chapter 6 - Biomaterials for Bioprinting (L. G. Zhang, J. P. Fisher, & K. W. B. T.-3D B. and N. in T. E. and R. M. Leong, Eds.)*. In . doi:10.1016/B978-0-12-800547-7.00006-0.

Ng, K. W., Leong, D. T. W., & Hutmacher, D. W. (2005). The challenge to measure cell proliferation in two and three dimensions. *Tissue Engineering, 11*(1–2), 182–191. https://doi.org/10.1089/ten.2005.11.182

Qin, C., Li, H., Xiao, Q., Liu, Y., Zhu, J., & Du, Y. (2006). Water-solubility of chitosan and its antimicrobial activity. *Carbohydrate Polymers, 63*(3), 367–374. https://doi.org/10.1016/j.carbpol.2005.09.023

Rickett, T. A., Amoozgar, Z., Tuchek, C. A., Park, J., Yeo, Y., & Shi, R. (2011). Rapidly photo-cross-linkable chitosan hydrogel for peripheral neurosurgeries. *Biomacromolecules, 12*(1), 57–65. https://doi.org/10.1021/bm101004r

Rosellini, E., Cristallini, C., Barbani, N., Vozzi, G., & Giusti, P. (2009). Preparation and characterization of alginate/gelatin blend films for cardiac tissue engineering. *Journal of Biomedical Materials Research Part A, 91A*(2), 447–453. https://doi.org/10.1002/jbm.a.32216

Ross-Murphy, S. B. (1992). Structure and rheology of gelatin gels: Recent progress. *Polymer, 33*(12), 2622–2627. https://doi.org/10.1016/0032-3861(92)91146-S

Seo, J. W., Shin, S. R., Lee, M.-Y., Cha, J. M., Min, K. H., Lee, S. C.Bae, H., … (2021). Injectable hydrogel derived from chitosan with tunable mechanical properties via hybrid-crosslinking system. *Carbohydrate Polymers, 251*, Article 117036. https://doi.org/10.1016/j.carbpol.2020.117036

Sung, H. W., Huang, R. N., Huang, L. L., & Tsai, C. C. (1999). In vitro evaluation of cytotoxicity of a naturally occurring cross-linking reagent for biological tissue fixation. *Journal of Biomaterials Science. Polymer Edition, 10*(1), 63–78. https://doi.org/10.1163/156856299x00289

Tsuji, Y., Li, X., & Shibayama, M. (2018). Evaluation of mesh size in model polymer networks consisting of tetra-arm and linear poly(ethylene glycol)s. *Gels (Basel, Switzerland), 4*(2), 50. https://doi.org/10.3390/gels4020050

Unal, S., Arslan, S., Karademir Yilmaz, B., Kazan, D., Oktar, F. N., & Gunduz, O. (2020). Glioblastoma cell adhesion properties through bacterial cellulose nanocrystals in polycaprolactone/gelatin electrospun nanofibers. *Carbohydrate Polymers, 233*, Article 115820. https://doi.org/10.1016/j.carbpol.2019.115820

Yan, L.-P., Wang, Y.-J., Ren, L., Wu, G., Caridade, S. G., Fan, J.-B.Reis, R. L., … (2010). Genipin-cross-linked collagen/chitosan biomimetic scaffolds for articular cartilage tissue engineering applications. *Journal of Biomedical Materials Research. Part A, 95*(2), 465–475. https://doi.org/10.1002/jbm.a.32869

Zhang, Y., Wang, Q.-S., Yan, K., Qi, Y., Wang, G.-F., & Cui, Y.-L. (2016). Preparation, characterization, and evaluation of genipin crosslinked chitosan/gelatin three-dimensional scaffolds for liver tissue engineering applications. *Journal of Biomedical Materials Research. Part A, 104*(8), 1863–1870. https://doi.org/10.1002/jbm.a.35717

Zuidema, J. M., Rivet, C. J., Gilbert, R. J., & Morrison, F. A. (2014). A protocol for rheological characterization of hydrogels for tissue engineering strategies. *Journal of Biomedical Materials Research. Part B, Applied Biomaterials, 102*(5), 1063–1073. https://doi.org/10.1002/jbm.b.33088